2）血液学的検査

手術前、術後 2 週、屠殺時（4 週または 12 週）に橈側皮静脈より血液を採取した。赤血球数(RBC)、ヘモグロビン量(HGB)、ヘマトクリット値(HCT)、血小板数(PLT)、平均赤血球容積(MCV)、平均赤血球血色素量(MCH)、平均赤血球血色素濃度(MCHC)、白血球数(WBC)、白血球分画（リンパ球、好中球、好酸球、単球）、網状赤血球比率(RET)、プロトロンビン時間(PT)、活性化部分トロンボプラスチン時間(APTT)、フィブリノーゲン濃度(Fbg)を測定した。

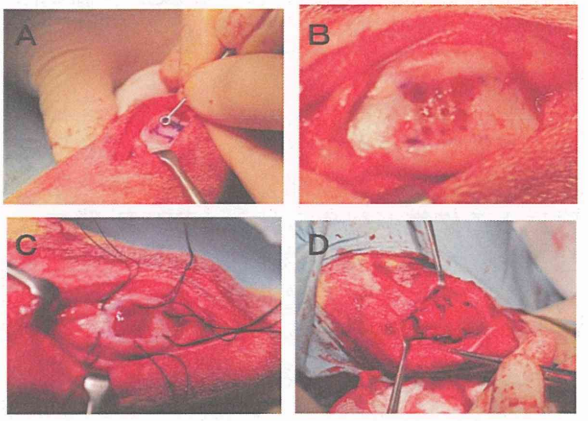

図 1　術中所見　A: 関節軟骨欠損作製　B: 骨髄刺激　C: 縫着用の骨孔作製　D: フィブロインによる関節軟骨欠損部の被覆

3）血液生化学的検査

同様に AST, ALT, ALP, CK,総コレステロール(T-Cho)、トリグリセリド(TG)、総タンパク(TP)、尿素窒素(UN)、クレアチニン(CRE)、総ビリルビン(T-Bil)、ブドウ糖(Glu)、無機リン(IP)、カルシウム(Ca)、ナトリウム(Na)、カリウム(K)、塩素(Cl)、タンパク分画、A/G 比、アルブミン(Alb)を測定した。

4）組織学的検討

術後 4 週および 12 週の時点で屠殺した動物の膝より、関節軟骨欠損部（大腿骨滑車）とその対側にあたる膝蓋骨を採取して、10%中性ホルマリン液にて固定、EDTA にて脱灰後、パラフィン切片を作成し、HE 染色、サフラニン O 染色及び II型コラーゲンに対する免疫組織染色を行った。欠損部の組織は ICRS（International Cartilage Repair Society）の Grading System により半定量的な評価を行った。

B－2：骨髄間葉系細胞播種＋フィブロイン被覆法

1）フィブロインの改良

前年度（平成 24 年度）の実験で、術中にフィブロインスポンジが縫合糸により裂けてしまうケースがあり、また、4 週の解剖時にすでに剥がれてしまっていたことから、固定操作や関節摩擦に対する強度の改善が必要と考えられた。そこで強度を増す目的で、フィブロインスポンジとフィブロインナノファイバーの複合化を行った（分担者玉田の研究報告書参照）。

これに伴い、フィブロインスポンジの厚みを 3mm から 1.5mm に変更した。細胞が入り込むのはフィブロインスポンジの表面 0.3mm 以内に限定されるため、細胞を保持するためには十分な厚さと考えられた。

2）骨髄由来間葉系幹細胞の採取

11～13 ヵ月齢雄のビーグル犬を用い、全身麻酔下に上腕骨近位に 16G の針を刺入して骨髄液 10ml を採取した。これを骨髄由来間葉系幹細胞分離デバイス（Kaneka）を通して、を採取した。細胞は細胞培養液で 0.5ml の細胞浮遊液とした後、フィブロインスポンジ上に滴下して播種した。このスポンジを軟骨欠損部の被覆に用いた。細胞を播種したフィブロインの一部はパラフィン標本として細胞の播種状態を確認した。

3）関節軟骨欠損モデルの作製

11～13 ヵ月齢雄のビーグル犬を用い、全身麻酔下に右膝蓋骨内側縁を切開し、膝蓋骨を外側に脱臼させ、大腿膝蓋関節の大腿骨側関節面に軟骨欠損（矢状方向: 12 mm x 冠状方向: 12 mm 程度）を作成した。

4）フィブロインによる関節軟骨欠損部被覆

関節軟骨欠損部の周囲に骨孔を 6 つ作成し、これらに糸を引き抜く形で、前述の改良型フィブロインスポンジ（X陽性糸を表層のナノファイバー層下に 1 本留置）を、軟骨欠損面に縫着した。細胞を播種していないフィブロインスポンジで被覆した対照群を F 群、骨髄由来間葉系幹細胞を播種したフィブロインスポンジで被覆した群を F+BMC 群とした。創を十分洗浄後、脱臼させた膝蓋骨を整復し、閉創した。

術後 3 日、1 週、2 週、4 週、12 週で右膝側

面像単純X線撮影を行った。手術後4週、12週に屠殺し（それぞれ各群n＝4）、局所状態、血液・生化学的検査、再生軟骨の肉眼所見の観察を行った。

4）血液学的検査、血液生化学的検査

手術前、術後2週、屠殺時（4週または12週）に橈側皮静脈より血液を採取した。赤血球数(RBC)、ヘモグロビン量(HGB)、ヘマトクリット値(HCT)、血小板数(PLT)、平均赤血球容積(MCV)、平均赤血球血色素量(MCH)、平均赤血球血色素濃度(MCHC)、白血球数(WBC)、白血球分画（リンパ球、好中球、好酸球、単球）、網状赤血球比率(RET)、プロトロンビン時間(PT)、活性化部分トロンボプラスチン時間(APTT)、フィブリノーゲン濃度(Fbg)を測定した

同様にAST, ALT, ALP, CK,総コレステロール(T-Cho)、トリグリセリド(TG)、総タンパク(TP)、尿素窒素(UN)、クレアチニン(CRE)、総ビリルビン(T-Bil)、ブドウ糖(Glu)、無機リン(IP)、カルシウム(Ca)、ナトリウム(Na)、カリウム(K)、塩素(Cl)、タンパク分画、A/G比、アルブミン(Alb)を測定した。

C．研究結果

C-1：骨髄刺激＋フィブロイン被覆法

1）歩行状態

いずれの群も術後より疼痛による歩行障害を認めたが、C群、BS群では術後14～19日で正常に回復した。一方、BS+F群は正常な歩行回復までに24日を要した。24日以降はいずれの群でも歩行異常は認められなかった。

2）血液・生化学的検査

いずれの項目も各群間で有意差は認めなかった。また、いずれの項目とも異常値は認めなかった。

3）軟骨欠損部の肉眼所見

術後4週では、軟骨欠損のみの対照(C)群ではほとんど修復を認めないが、骨髄刺激(BS)群では骨孔部に白色の修復組織が認められた。骨髄刺激＋フィブロイン(BS+F)群では欠損部は全体に白色の修復組織で覆われ、骨孔部分は陥凹している所見が認められた。

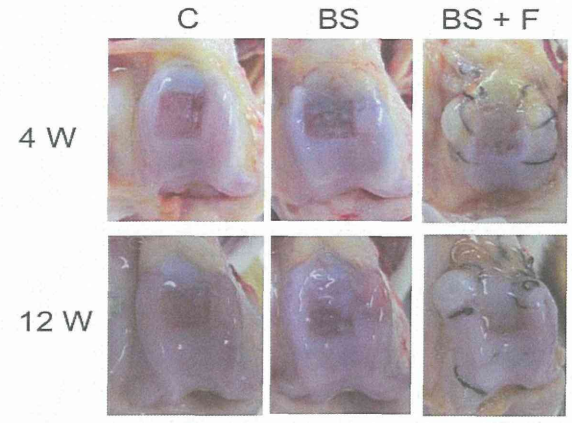

図2　術後4週および12週での軟骨欠損部の肉眼所見　C: 軟骨欠損のみ, BS: 骨髄刺激, BS+F: 骨髄刺激＋フィブロイン

術後12週では、C群では4週と同様にほとんど軟骨修復を認めなかったが、BS群では骨孔部周囲を中心に部分的に軟骨様の白色組織による修復が認められた。BS+F群では、BS群よりも広い範囲で修復が認められ、4週時に比べてより厚く光沢のある軟骨様組織で覆われていた。（図2、この結果は前年度の報告書においてもすでに報告済み）

4）軟骨欠損部の組織所見

術後4週では、BS+F群では他の2群と比較して軟骨欠損部に修復組織が認められていたが、この修復組織は、サフラニン0染色、Ⅱ型コラーゲン免疫染色ともに染色性不良であり、一部に軟骨様組織を認めるのみであった。軟骨欠損のみの対照(C)群では修復組織は認められず、BS群で骨孔部に認められた白色の修復組織も、サフラニン0染色、Ⅱ型コラーゲン免疫染色ともに染色されなかった。（図3）

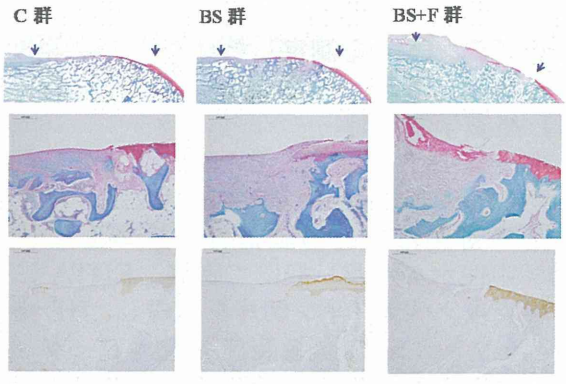

図3　術後4週の軟骨欠損部の組織像
C:軟骨欠損のみ, BS:骨髄刺激, BS+F:骨髄刺激＋フィブロイン、上段・中段：サフラニンO染色、下段：Ⅱ型コラーゲン免疫染色

術後 12 週では、BS+F 群において、サフラニン O 染色、II 型コラーゲン免疫染色で染色される修復組織が認められた。組織学的にはほとんどが線維軟骨の所見で、一部に硝子軟骨様組織を認めた。C 群では修復は認められず、BS 群では骨孔部にのみサフラニン O 染色、II 型コラーゲン免疫染色で染色される修復組織が認められた。（図４）

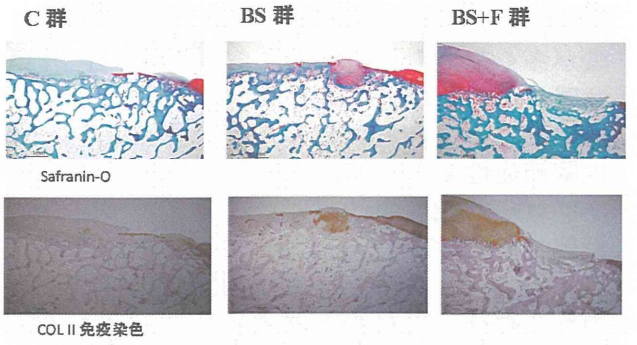

図４　術後 12 週の軟骨欠損部の組織像
C:軟骨欠損のみ, BS:骨髄刺激, BS+F:骨髄刺激＋フィブロイン、上段・中段：サフラニン O 染色、下段：II 型コラーゲン免疫染色

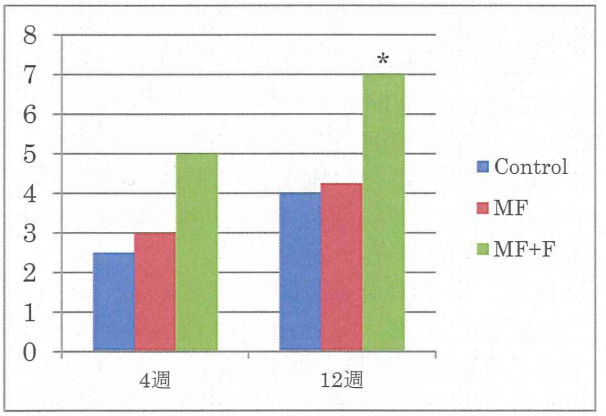

図５　ICRS scale による軟骨欠損部修復の半定量的評価

ICRS (International Cartilage Repair Society) の Grading System により半定量的な評価を行ったところ、12 週の BS+F 群において、他群と比較して有意な改善が認められた（*)。

C-2：骨髄間葉系細胞播種＋フィブロイン被覆法

1）歩行状態
F 群、F+BMC 群とも術後より疼痛による歩行障害を認めたが、術後 21 日以降には歩行異常は認められなかった。

2）血液・生化学的検査
いずれの項目も各群間で有意差は認めなかった。また、いずれの項目とも異常値は認めなかった。

3）X線学的検査
フィブロインスポンジ表層に縫いこんだX線陽性糸の観察では、F 群、F+BMC 群とも、4 週、12 週の飼育期間の間、フィブロインスポンジはほぼ軟骨欠損部上にとどまっていた。しかし、4 週くらいから軟骨欠損部の軟骨下骨の融解像が認められるようになり、12 週では同部の骨欠損、周囲の硬化像など変形性関節症性の変化が起きていた。

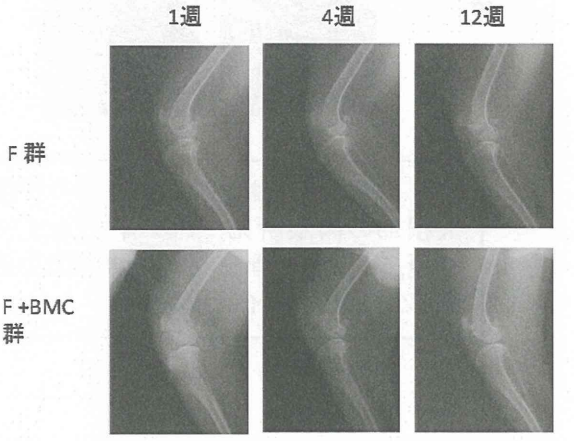

図６　術後単純X線 右膝側面像

4）骨髄細胞を播種したフィブロインスポンジの組織像
F+BMC 群のフィブロインスポンジ内には骨髄由来細胞が認められた。

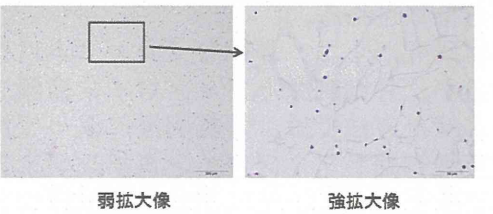

図７　フィブロインスポンジ内の骨髄由来細胞（HE 染色）

5）軟骨欠損部の肉眼所見

術後 4 週では、F 群比較して、F+BMC 群では欠損部に白色の修復組織が多く認められる傾向にあった。しかし、12 週時には両群ともに変形性関節症性変化の進行が認められ、肉眼的には軟骨欠損部の修復に明らかな差は認められなかった。

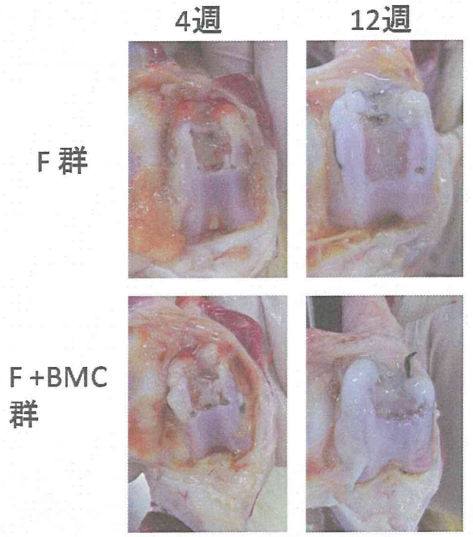

図 8　術後 4 週および 12 週での軟骨欠損部の肉眼所見　F:フィブロイン被覆, F+BMC: 骨髄間葉系幹細胞を播種したフィブロイン被覆

D．考察

本研究の結果から、イヌなどの大型動物においても、フィブロインが関節軟骨の修復に促進的な役割を果たすことが示された。我々は、軟骨細胞はフィブロインの中で細胞凝集体を形成し基質合成を行うこと、そしてこれらの凝集体は生体内で周囲に移動して軟骨組織形成に寄与することを明らかにしてきた（フィブロインの cell delivery 機能）が、今回の動物モデルにおいても同様の機序が働いたと推察される。

本研究からは、詳細なメカニズムは不明であるが、骨髄刺激とフィブロイン被覆を組み合わせた方法では、骨髄刺激によって流出した骨髄細胞がフィブロインスポンジ上で細胞凝集体を形成し、それが軟骨欠損部に白色の修復組織形成を促したと考えられる。そして、術後 12 週においてこれらの組織は軟骨細胞へ分化していた。骨髄刺激法とフィブロインスポンジ被覆を併用する方法は、広範囲関節軟骨欠損の治療の応用できる可能性がある。

さらに、より高い軟骨再生効果を得る手段として、骨髄内の未分化間葉系幹細胞を濃縮してフィブロイン内に効率よく播種し、欠損部へ移植する方法が考えられる。そこで、関節軟骨欠損部に、骨髄間葉系幹細胞（専用フィルターにより分離）を播種したフィブロインスポンジを被覆する方法を試みた。

この実験では、術後 4 週で骨髄間葉系幹細胞播種群において軟骨欠損部に白色の修復組織が多く認められる傾向にあったが、12 週では明らかな差は認められなかった。また、この時点では両群ともに軟骨下骨の骨破壊や変形性関節症性変化の進行がみられた。これは、フィブロイン強度を改良し、フィブロインの欠損部への固定性を向上させたことで、フィブロインが 12 週間という長期間にわたって欠損部に存在したためと考えられた。フィブロインが長期間にわたって関節面に機械的負荷を与えると、軟骨欠損部の修復には悪影響を与える可能性が示唆された。

また、フィブロインに分離した骨髄間葉系幹細胞を播種するだけでは細胞数が不十分であった可能性があり、骨髄刺激法と分離骨髄細胞の播種を併用する方法も有効ではないかと考えられた。

次年度（平成 26 年度）は、フィブロイン被覆をあえて短期間（2 週間）として、フィブロインによる関節面への機械的負荷を軽減し、かつ骨髄刺激法と分離骨髄細胞の播種を併用することで、より優れた軟骨再生効果が得られるかを検証する予定である。

また、ヒトの骨髄細胞、軟骨細胞（人工関節手術時に採取、院内倫理委員会の承認を得てすでに採取、培養を開始済み）をフィブロインスポンジ内で培養し、小動物を用いた実験結果と同様の細胞凝集体形成や軟骨組織形成がみられるかどうかを、in vitro の系を用いて確認する予定である。

これらの結果を踏まえて、現在有効な治療法のない若年者変形性関節症における広範囲軟骨欠損に応用していくことを検討している。

E. 研究発表

１．論文発表

０件

２．学会発表

６件

１）中川晃一、富田直秀、玉田 靖、平方栄一、青木秀之、園部正人、柴田孝史、中島 新、齋藤知行：フィブロインの cell delivery 機能を利用した関節軟骨再生法の開発．第５回日本関節鏡・膝・スポーツ整形外科学会（JOSKAS），（シンポジウム；軟骨再生医療の最前線），札幌，2013.6.20-22

２）中川晃一、富田直秀、玉田 靖、中島 新、柴田孝史、園部正人、北原聡太、青木保親、高橋 宏、齋藤雅彦、谷口慎治、山田 学、平方栄一、青木秀之、齋藤知行：広範囲関節軟骨欠損に対する骨髄刺激とフィブロイン被覆の併用療法の効果．第41回日本関節病学会（パネルディスカッション；OA の病態を考慮した治療の基礎と臨床），名古屋，2013.11.2-3

３）中川晃一、富田直秀、玉田 靖、柴田孝史、園部正人、中島 新、青木保親、平方栄一、青木秀之、齋藤知行．イヌ広範囲関節軟骨欠損の修復過程におけるフィブロイン被覆法の初期効果．第28回日本整形外科学会基礎学術集会，千葉，2013.10.17-18

４）青木秀之、富田直秀、川上雅弘、中村卓司、宮崎芳安、柘植新太郎、宍倉 亘、玉田 靖、中川晃一、土谷一晃．絹フィブロインスポンジの孔径が再生軟骨の組織形成に及ぼす影響．第28回日本整形外科学会基礎学術集会，千葉，2013.10.17-18

５）平方栄一、富田直秀、玉田 靖、勝呂 徹、中嶋正明、神戸裕介、山本浩司、川上雅弘、大高晋之、奥村秀雄、鈴木茂彦．ウサギ膝蓋骨全範囲の骨軟骨欠損に対するフィブロインスポンジ被覆法による早期組織修復．第28回日本整形外科学会基礎学術集会，千葉，2013.10.17-18

６）中川晃一：シルク・フィブロインを利用した関節軟骨再生法の開発．第15回千葉スポーツ医科学研究会，千葉，2014.5.9

Ｆ．知的財産権の出願・登録状況

１．特許取得

０件

２．実用新案登録

０件

厚生労働科学研究費補助金（医療技術実用化総合研究事業）
（分担）研究報告書

内側楔状開大式高位脛骨骨切り術後の軟骨修復に関する研究

分担研究者　齋藤知行　横浜市立大学医学部整形外科　教授

研究要旨
高位脛骨骨切り術にフィブロインスポンジ移植を併用することを検討している。適応や対象症例の選択を含めた治療ガイドラインを作成するにあたり、高位脛骨骨切り術単独での軟骨修復について評価を行った。Opening wedge 法では Closed wedge 法に比較して修復は劣っていた。修復に影響する因子として、部位、変性 Grade、性別、BMI が関与した。

A．研究目的

変形性膝関節症(OA)に対する関節温存術式として高位脛骨骨切り術(HTO)がある。HTO 術後に一部の症例では関節軟骨の修復反応が観察されるが、一方で修復困難な例も多く存在する。HTO にフィブロインスポンジ移植を併用することで OA 患者の関節軟骨修復を促進することが期待されるが、治療の対象を含めたガイドライン作成が必要と考える。HTO 術後の軟骨修復を評価し、修復に影響を与える因子について検討することが本研究の目的である。

昨年度は従来行われてきた Closed wedge 法による HTO 術後の軟骨修復について検討を行った。今年度は最近の Opening wedge 法による HTO を施行した症例を対象に検討を行った。

B．研究方法

1）対象

OA の診断で OWHTO を行った 84 例 114 膝（平均年齢 66 歳、男性 39 膝、女性 75 膝）である。本術式の適応として、病変が内側に限局され、かつ術前の膝屈曲拘縮が 15° 未満、矯正角度が 15° 未満の症例を対象とした。

2）術式

脛骨近位内側で関節面より 3.5mm の部位から近位脛腓関節へ向かう斜め骨切りを行った。骨切り部は目標に矯正角度まで楔状に開大し、開大部には人工骨のブロックを挿入した。骨切り部の固定は TomoFix プレートを用いた（図 1）。

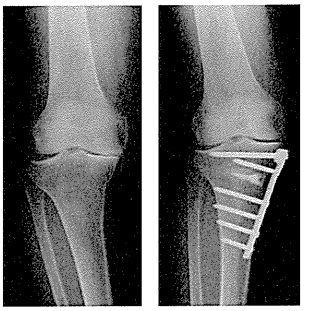

術前　　術後

図 1　Opening wedge HTO

3）評価

臨床的評価として術前・術後の日本整形外科学会膝疾患治療成績判定基準（JOA スコア）および立位膝単純 X 線正面像における膝外側角(femorotibial angle, FTA)を調査した。

関節軟骨の評価は術前および術後抜釘時に関節鏡にて行った。術前の軟骨変性は International Cartilage Repair Society (ICRS)の grade 分類で評価した。術後の軟骨修復は以下の分類に従って評価した（図 2）。

Stage 1: 修復の変化が全くないか、あってもごくわずかな変化のみ観察されるもの
Stage 2: 軟骨欠損部を部分的に被覆するもの
Stage 3: 軟骨欠損部を全体的に被覆するもの

Stage 1　　Stage 2　　Stage 3

図 2　関節軟骨修復の Stage 分類

C．研究結果

1）臨床成績

JOA スコアは術前平均 65 点から術後 1 年で平均 91 点に改善した(P<0.05)。立位 FTA は術前平均 182.2° から術後平均 169.5° に変化した(P<0.05)。

2）関節軟骨の評価

術前の軟骨変性は、大腿骨側が Grade 1：10 膝(9%)、2：46 膝(40%)、3：58 膝(51%)、脛骨側が Grade 1：12 膝(11%)、2：52 膝(45%)、3：50 膝(44%)に分類された。

術後の軟骨修復は、大腿骨側が Stage 1：33 膝(29%)、 2：63 膝(55%)、 3：18 膝(16%)、脛骨側が Stage 1：58 膝(51%)、2：49 膝(43%)、3：7 膝(6%)に分類され、部分的あるいは全体的に修復された膝数は大腿骨の方が有意に多かった。

3）軟骨修復に影響する因子

年齢、性別、BMI、術前 ICRS grade、術後立位 FTA の各因子と軟骨修復の影響を検討した。

大腿骨側では、Stage2 以上の修復は ICRS Grade の進行した症例に多くみられ、Stage3 は男性に多くみられた。脛骨側では Stage2 以上の修復は BMI25 未満の症例において多くみられた。年齢および術後立位 FTA では有意な差はみられなかった。

D．考察

白色の軟骨様組織による大腿骨側軟骨欠損部の完全被覆は、Close wedge HTO では 32%の症例において確認されたのに対し、Opening wedge HTO では 16%の症例にみられるのみであった。今回の結果から大腿骨側では術前の変性 Grade の進行した症例の方が修復は良好であったが、Closed wedge 法の適応になる症例の方が Opening wedge 法の例に比較して Grade の進行した例が多く、この違いが修復の差に関与した可能性が考えられる。それ以外では Opening wedge 法では開大により内側の軟部組織の緊張が強くなる等、術式の違いによる因子も考えられるが、メカニズムは不明であり、今後の検討課題でもある。

今回の結果より Opening wedge HTO 術後の軟骨修復に影響を与える因子は部位、ICRS Grade、性別、BMI であり、年齢や術後 FTA には影響されないことが分かった。ただし、本症例の術後 FTA については、175° 以上の矯正不足症例は 3 例のみであるため、判断には注意を要すると思われる。

E．結論

Opening wedge HTO 術後の軟骨修復がみられる症例は少なく、修復を促進する目的としてフィブロインスポンジ移植は有効な手段に成り得ると考えられる。特に修復不良因子を有する症例では適応するのが望ましいと考えられた。今後はさらに詳細に修復に影響する因子について検討を重ね、治療ガイドラインに反映させる予定である。

F．研究発表

1．論文発表

0 件

2．学会発表

0 件

G．知的財産権の出願・登録状況

1．特許取得

0 件

2．実用新案登録

0 件

3．その他

III. 研究成果の刊行に関する一覧表

雑誌

発表者氏名	論文タイトル名	発表誌名	巻号	ページ	出版年
Otaka A., Kachi N.D., Hatano N., Kuwana Y., Tamada Y., Tomita N.	Observation and quantification of chondrocyte aggregation behavior on fibroin surfaces using Voronoi partition	Tissue Engineering Part C Methods	19(5)	396-404	2013

TISSUE ENGINEERING: Part C
Volume 19, Number 5, 2013

DOI: 10.1089/ten.tec.2012.0424

Observation and Quantification of Chondrocyte Aggregation Behavior on Fibroin Surfaces Using Voronoi Partition

Akihisa Otaka, MEng,[1] Naoyoshi D. Kachi, PhD,[1] Naoya Hatano, BE,[1] Yoshihiko Kuwana, PhD,[2] Yasushi Tamada, PhD,[2] and Naohide Tomita, MD, PhD[1]

Cell migration is one of the fundamental processes in histogenesis, and it is necessary to investigate such multicellular behavior quantitatively in cell regeneration studies. In this study, Voronoi diagram analysis was first confirmed in simulation testing, and then used to evaluate the multicellular behavior of chondrocytes on three different substrates: (1) wild-type fibroin (FIB); (2) L-RGDSx2 transgenic fibroin; (3) and collagen. The indices for the round factor average, round factor homogeneity, and area disorder (AD), calculated from Voronoi diagram analysis, were used to characterize the difference in spatiotemporal changes for the different chondrocyte populations, and a regression analysis of the AD index was used to measure the speed of cell aggregation. The results suggested that the arginine-glycine-aspartic acid-serine sequence affects aggregate formation of chondrocytes cultured on FIB. The Voronoi diagram analysis represents one of the promising quantitative analyses for cell regeneration studies.

Introduction

Live-cell observation has become a powerful analytical tool in many cell biology laboratories because of advancements in microscopy techniques and cell imaging technologies.[1] On the other hand, evaluation methods for quantifying multicellular morphodynamics are still not yet fully developed. However, to successfully engineer artificial tissue constructs, some quantification tools for analyzing multicellular formation are necessary.[2]

For accurately evaluating the spatiotemporal formation of cell populations, there are two major requirements. First, automated visual tracking of the cells is necessary for quantitative and systematic analysis. Second, techniques that accurately characterize patterns of cell behavior, such as migration, proliferation, and apoptosis, are required. While visual tracking techniques have been studied extensively, less attention has been given to cell behavior characterization techniques.

In previous work, Kawakami *et al.* demonstrated that initial chondrocyte aggregation led to enhanced cartilage tissue formation in fibroin (FIB) sponges.[3] Additionally, cell aggregation is considered to be a key event in a wide range of fields, from tissue engineering to embryology and involves many types of cells, such as hepatocytes and chondrocytes,[3–5] as along with tumor and mesenchymal stem cells as well. This indicates that cell aggregation is one of the key events in cell-to-cell interaction, making it a vital part of tissue formation. However, in multicellular biophysics, evaluation of the cell aggregation process has been neither quantitative nor objective, but rather qualitative and highly researcher dependent. This lack of reliable and repeatable quantitative cell aggregation assays has made it difficult to investigate multicellular biophysics in the aggregate formation process.

The purpose of this study was to introduce the concept of "cellular sociology" into tissue engineering and bioenvironment design. This concept focuses on the social behavior of cell populations, which varies in response to the cells' surroundings and the physiological and phenotypical state of the cells themselves. Moreover, by understanding the relationship between cell population and extracellular environment, it is possible to gain insights into a wide range of cell biophysics (e.g., cell–cell and cell–substrate/material interactions). In the field of cellular sociology, cell arrangement analysis using a Voronoi diagram is one of the most successful methods for the evaluation of different cell populations. Voronoi analysis has been used previously to evaluate the spatiodistribution of retinal,[6] cortical,[7] and tumor cells.[8–11] Nawrocki Raby *et al.* evaluated the process of tumor cell cohesion using graphical quantification, including Voronoi diagram analysis, and concluded that this method represented a new way to predict the aggressiveness of various tumor cells.[9] In a similar fashion, Voronoi diagram analysis may provide new insights into the multicellular biophysics involved in tissue regeneration and allow for improved computational modeling of cell behavior in scaffolds.

[1]Department of Mechanical Engineering and Science, Kyoto University Graduate School of Engineering, Kyoto, Japan.
[2]National Institutes of Agrobiological Sciences, Tsukuba, Japan.

In this study, two types of experiments were performed. First, Marcelpoil and Usson's distribution assay,[12] which has been used in the study of tumor cell distribution,[9,11] was examined with respect to its validity as a method for evaluating chondrocyte aggregation on different substrates. Specifically, to confirm the relationship between cell aggregation and various analysis metrics, unambiguous examples of different aggregation patterns were simulated and analyzed in a set of *in silico* experiments. After confirming these relationships, a number of *in vitro* experiments were then performed to examine the spatiotemporal distributions of chondrocytes on three different substrates: (1) collagen (CON); (2) FIB; and (3) RGD-transgenic fibroin, which was created by genetically interfusing arginine-glycine-aspartic acid-serine (RGDS) peptides into silk FIB molecules.[13] It was reported previously that chondrocyte aggregation is enhanced in FIB sponges,[3] but chondrocyte aggregation behavior on FIB has yet to be evaluated quantitatively. Thus, the objective of this study was to quantitatively assess whether FIB enhances cell aggregation behavior using *in silico* validated Voronoi diagram analysis methods.

Materials and Methods

Cell population quantification

The spatial distribution of cells was characterized and quantified using a cellular sociology algorithm based on geometrical models, as described by Marcelpoil and Usson[12] (i.e., Voronoi's partition). These methods, applied to the set of points that relate to the position of the cells (Fig. 1), provide information about the spatial distribution and neighborhood relationships of the cells. From the Voronoi diagram, three quantitative parameters can be deduced: (1) average and standard deviation of the areas (round factor average [RFav]); (2) roundness factor homogeneity (RFH); and (3) area disorder (AD). Each index was calculated using the equations derived by Marcelpoil and Usson.[12] As is customary, border zones of the Voronoi diagram were excluded from the analysis, as no information can be taken relating to the final position of cells in these zones.

In silico *experiment: simulation of aggregate cell populations*

Model formulation. Cell aggregations can vary in their size, cell density, and gathering potential. A computer simulation model was conducted to examine whether cell population affects the RFav, RFH, and AD indexes during aggregation. Three cell population models (type A, type B, and type C; described in section "Model of cell arrangement") that were observed regularly in our time-lapse observation were simulated. Afterward, the cell distribution points were evaluated using a Voronoi diagram. Every trial was executed and evaluated six times.

Model of cell arrangement. Three types of cell distribution were created using 100 separate points set on a 2D plane using the procedures described below. (Note: Cells were not placed at the exact nodal points of the square lattice, but rather randomly scattered around each node using a Gaussian distribution with a standard deviation of 10 pixels (Fig. 2).

Type A: This model was used to analyze the effect of cell density. Using a 10×10 array of points located at the nodes of a perfect square lattice, groups with high, medium, and low cell density were simulated by changing the mesh size of the square lattice to 30 (high density; H), 60 (middle density; M), and 90 pixels (low density; L), respectively. A control group (C) in which the population was distributed randomly (Fig. 3, model A) was also created.

Type B: This model was used to evaluate the rate at which cells participated in aggregation. Using an array of N points located at the nodes of a square lattice and 100-N points distributed randomly, groups with 0%, 25%, 50%, 75%, and 100% aggregation participation ratios were simulated by changing the N value to 0, 25, 50, 75, and 100, respectively (Fig. 3, model B).

Type C: This model was used to analyze the effect of aggregate size. Using point forming groups, three types of cell populations were created in which cells formed: one large aggregate (AGG:1); two smaller aggregates (AGG:2); and four aggregates (AGG:4) that were smaller still. Each nodule

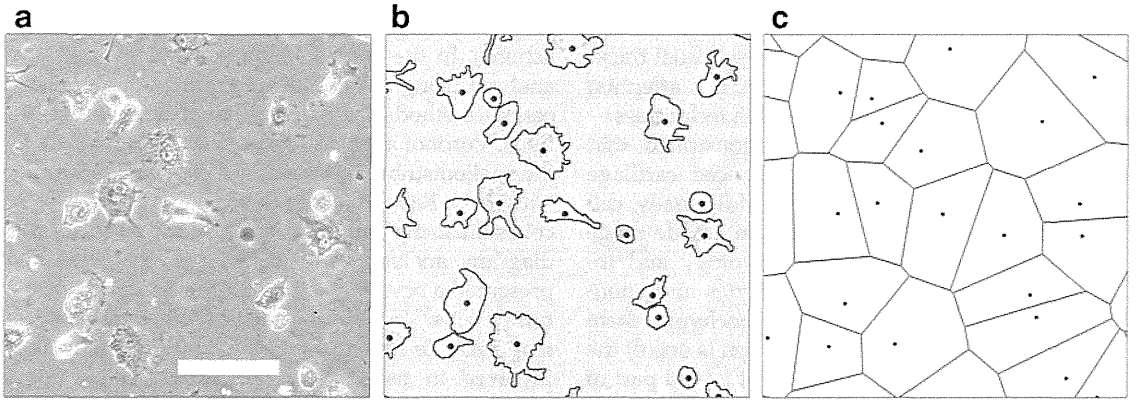

FIG. 1. Representation of the data acquisition process. **(a)** Example of typical cartilage observation on a polydimethylsiloxane surface with a phase-contrast microscope. **(b)** Outlines and center points of cells extracted from snapshot images. **(c)** The derived Voronoi polygon using the point set of cell centers created by the Open Computer Vision Library (http://opencv.willowgarage.com/wiki/). Scale bar = 20 μm.

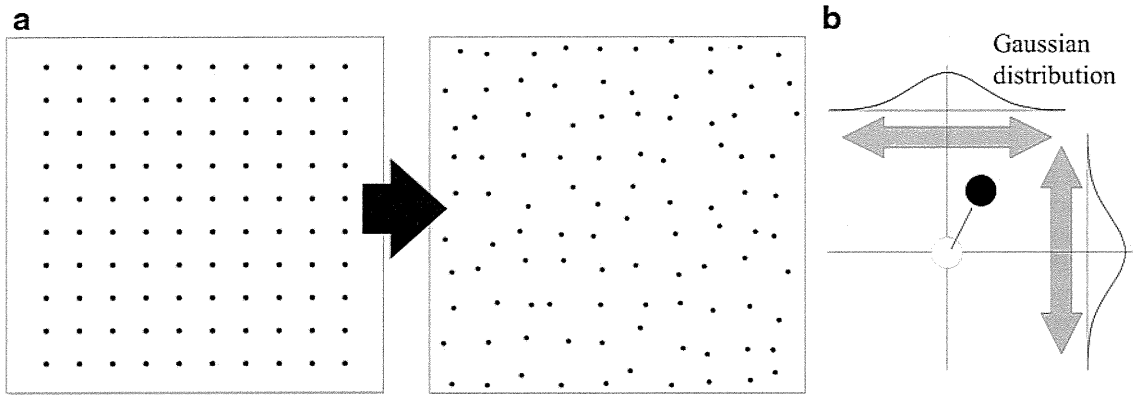

FIG. 2. Schematic model of an aggregating cell population. **(a)** Randomization of the point set ordered at the nodes of a square lattice. **(b)** Spatial perturbation of a point in XY coordinates according to the Gaussian distribution with a standard deviation of 10 pixels.

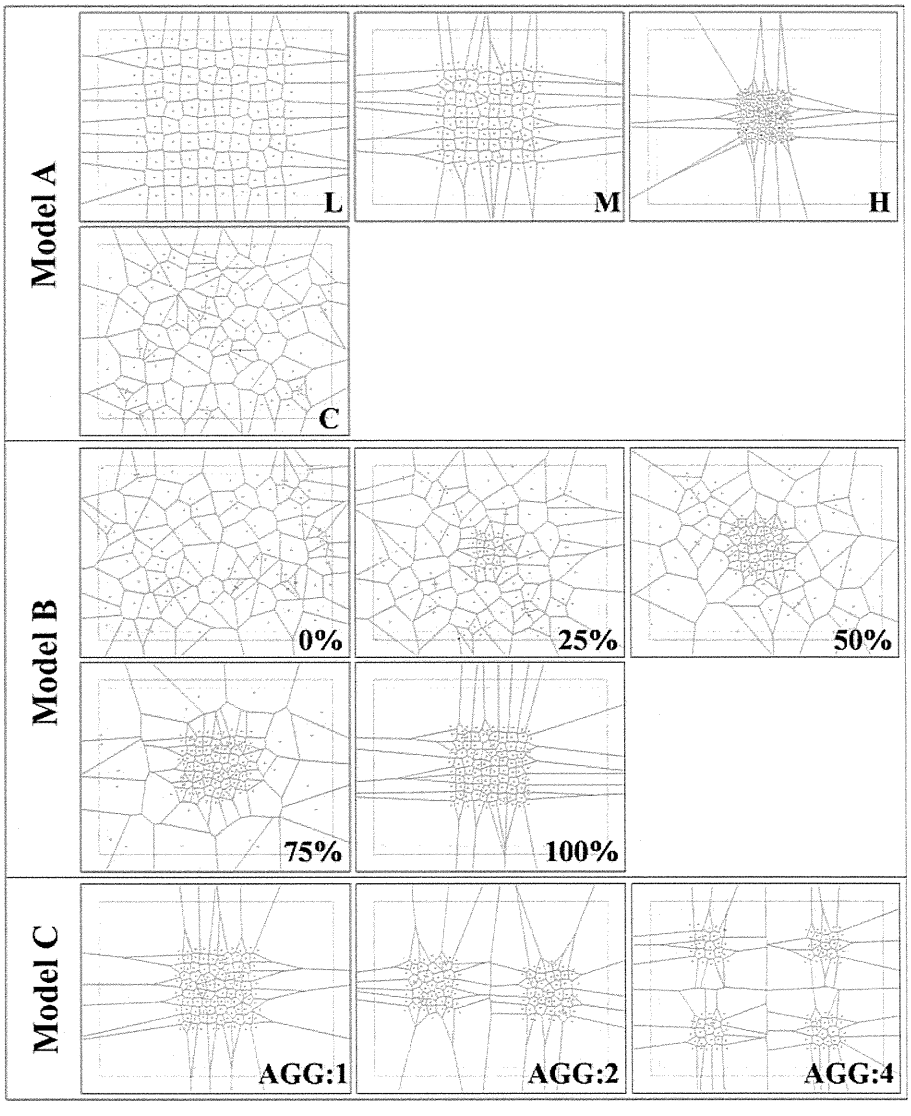

FIG. 3. Representative image of aggregation models. Each model was varied in the degree of cell density (type A), cell aggregation participation ratio (type B), and the number of cells within each aggregrate (type C).

had the same size and contained 100, 50, and 25 points, respectively (Fig. 3, model C).

In vitro *experiment: cell seeding experiment in 2D culture*

Chondrocyte preparation. Articular cartilage tissue was aseptically removed from the proximal humerus, distal femur, and proximal tibia of 4-week-old Japanese White rabbits (Oriental Bio Service Co., Ltd.). After any adherent connective tissue had been removed, the excised cartilage tissue was diced into 1-mm^3 segments and chondrocytes were isolated by digesting small segments of cartilage with 0.25% trypsin-ethylenediaminetetraacetic acid (EDTA) (Nacalai Tesque, Inc.) for 30 min in a temperature-controlled bath at 37°C. After being rinsed twice with Dulbecco's phosphate-buffered saline (PBS; Nacalai Tesque, Inc.) and centrifuged at 1500 rpm for 5 min, the cartilage was enzymatically digested with 0.25% type II collagenase (CLS-2; Worthington Biochemical Co.) for 6 h at 37°C. After staining through a cell strainer (BD Falcon, Inc.) and washing twice with PBS, a single-cell suspension was obtained. Cartilage harvests from living animals were approved and accepted by the animal care committee of the Institute for Frontier Medical Sciences at the Kyoto University.

Cells were passaged once in T-flasks (Iwaki Glass Co., Ltd.) with the Dulbecco's modified Eagle's medium (DMEM; Nacalai Tesque, Inc.) containing 10% fetal bovine serum (FBS; Nacalai Tesque, Inc.) and 1% antibiotic mixture (10,000 U/mL penicillin, 10,000 mg/mL streptomycin, and 25 mg/mL amphotericin B; Nacalai Tesque, Inc.) before experimentation. Cells were cultured at 37°C in a humidified atmosphere of 95% air and 5% CO_2 for 5 days, and the medium was changed every 2 days.

Substrate preparation. A polydimethylsiloxane (PDMS) liquid solution was prepared by using a SYLGARD 184 SILICONE ELASTOMER KIT (Dow Corning Toray Co., Ltd.) and curing for 48 h at room temperature in a culture dish (diameter, 150 mm; Asahi Glass Co., Ltd.). Afterward, the PDMS sheet was cut into disks that were 2 mm in thickness and 35 mm in diameter. Disks were sterilized by autoclave before experimentation.

CON, wild-type FIB, and L-RGDSx2 fibroin (LRF) were used as substrate coatings and prepared using the procedures listed below. Three substrate-coated disks were prepared for each substrate (CON, FIB, and LRF) and set in a culture dish (diameter, 35 mm; Asahi Glass Co., Ltd.). Each substrate disk was washed twice with PBS before use.

CON substrate: As a control, type I collagen-coated PDMS disks were used, with PDMS chosen due to its hydrophobic nature. The PDMS disks were soaked in 10% Cellmatrix Type I-C (Nitta gelatin, Inc.) diluted in HCl (pH 3.0, 1 mM) for 30 min at room temperature. Afterward, the plates were washed with a culture medium (DMEM) three times and with PBS twice thereafter.

FIB substrate: A FIB aqueous solution was prepared as described previously.[5,14] Briefly, degummed silk FIB fibers from *Bombyx mori* cocoons were dissolved in a 9 M lithium bromide aqueous solution at room temperature, with the solution subsequently dialyzed against pure water. The concentration of FIB in the water solution was determined by the colorimetric method and was prepared to be 1% (wt/vol). Before coating the FIB substrate, PDMS disks were treated with O_2 plasma to make the surface hydrophilic. The PDMS disks were then soaked in the FIB aqueous solution for 1 h at room temperature and dried at 50°C. The coated disks were immersed in an 80% methanol solution for 1 h and dried again at 50°C.

LRF substrate: The LRF is a protein in which (RGDS)x2 sequences have been fused with FIB L-chains at the amino-terminus. An LRF aqueous solution was prepared using the same technique as that used for the preparation of the wild-type FIB aqueous solution. PDMS disks coated with LRF were also manufactured in the same process as that used for the wild-type FIB samples.

Time-lapse microscopy. Passaged chondrocytes were removed from T-flasks by adding 0.25% trypsin-EDTA and washing twice with PBS. Shortly after detachment, cells were suspended in the Leibovitz's L-15 medium (Invitrogen Corp.) containing 10 vol% FBS, and 1 vol% antibiotic mixture and seeded on substrate dishes at a concentration of 1.5×10^4 cells/cm^2. Following that, the dish was placed on an inversion microscope (IX-71; Olympus Corp.) and enclosed in a small transparent culture chamber (MI-IBC-IF; Olympus Corp.) with in a humidified atmosphere at 37°C. A 10× magnification objective lens (CPlan N 10x/0.25 PhC; Olympus Corp.) was used in our experiment. During a 24-h culture, time-lapse phase-contrast images were captured every 10 min by a CCD camera (DP70; Olympus Corp.).

Chondrocyte distribution quantitation. To acquire positional datum related to the chondrocytes' distribution, the images, captured at 10 min, and 3, 6, 9, 12, and 24 h after seeding, were analyzed according to the following procedure. Each cell was outlined and painted over manually using Photoshop (Adobe Systems, Inc.) and cell binary images were generated. Afterward, the cell positions were sorted out using the Particles Analysis command in ImageJ (National Institutes of Health) (Fig. 1). Using this population data, Voronoi diagrams were produced and three indexes (AD, RFav, RFH) were calculated. The number of cells was also recorded, and the rate of cell growth was calculated by dividing the number of cells in each time step by the initial number of cells. Time-dependent changes in AD were fitted to a nonlinear regression model.

Statistical analysis and data presentation

Experimental values in each figure are presented as mean ± standard deviation. One-way analysis of variance (ANOVA) and a Tukey's test for *post hoc* comparison were done to analyze the significance of time-dependent changes in RFH, RFav, AD, and the rate of cell growth in *in vitro* experiments. A Student's *t*-test was done to analyze the significance between the groups in the *in vitro* experiment. All statistical tests were determined using a criterion of $p < 0.05$. An asymptotic exponential curve was used for regression analysis of the temporal AD changes on each substrate.

Results

The outcomes from in silico *experiments*

The RFav versus RFH versus AD shown in Figure 4 describes the results for RVav, RFH, and AD in the *in silico* experiments. These results were calculated from cell simulations

using type A (Fig. 4a), type B (Fig. 4b), and type C (Fig. 4c) cell populations. In these conditions, RFav, RFH, and AD ranged from 0.65 to 0.80, from 0.74 to 0.90, and from 0.31 to 0.72, respectively.

The statistical significance analysis indicates that RFav is insensitive to the rate at which cells participate in aggregation (Fig. 4b), and that RFH is insensitive to the number of cells involved in aggregation (Fig. 4c). On the other hand, AD results reveal a significant difference between multiple groups for all simulation types. Thus, AD appears to be more sensitive than RFav and RFH in evaluating aggregating cell populations, especially with respect to aggregate cell density and the ratio of cells involved in aggregation.

The outcomes from in vitro *experiments*

In Figure 5, chondrocytes on each substrate are shown after 12 and 24 h of culture time. On the CON substrate, chondrocytes elongated and few cells were found to be in contact with each other (CON). On both FIB substrates (FIB and LRF), most chondrocytes maintained a rounded shape and participated in cell aggregation. Chondrocytes on these substrates were active in migration during the early stages of cell culture, but cell speed appeared to decrease with cell aggregation. Compared with the LRF substrate, the aggregation size was larger and fewer cells remained solitary on the FIB substrate.

Chondrocytes on the FIB and LRF substrates did not increase significantly in the 24-h culture period, as shown in Figure 6. Only on the CON substrate was significant cell growth observed ($p < 0.01$, one-way ANOVA). Furthermore, significant differences in the temporal cell growth on the CON substrate were found only between 10 min–24 h ($p < 0.01$), 3–24 h ($p < 0.01$), and 12–24 h ($p < 0.05$, Tukey test) of culture time. Thus, there were no significant changes in cell proliferation during the first 12 h after seeding on each surface.

The time-dependent changes in RFav, RFH, and AD for chondrocytes grown on each substrate are shown in Figure 7. The initial value for each index was almost the same for each substrate, but the RFav and AD values for the FIB substrate and all three indices for the LRF substrate changed significantly over the 24-h culture period ($p < 0.05$, one-way ANOVA). The absence of change in the indexes recorded for the

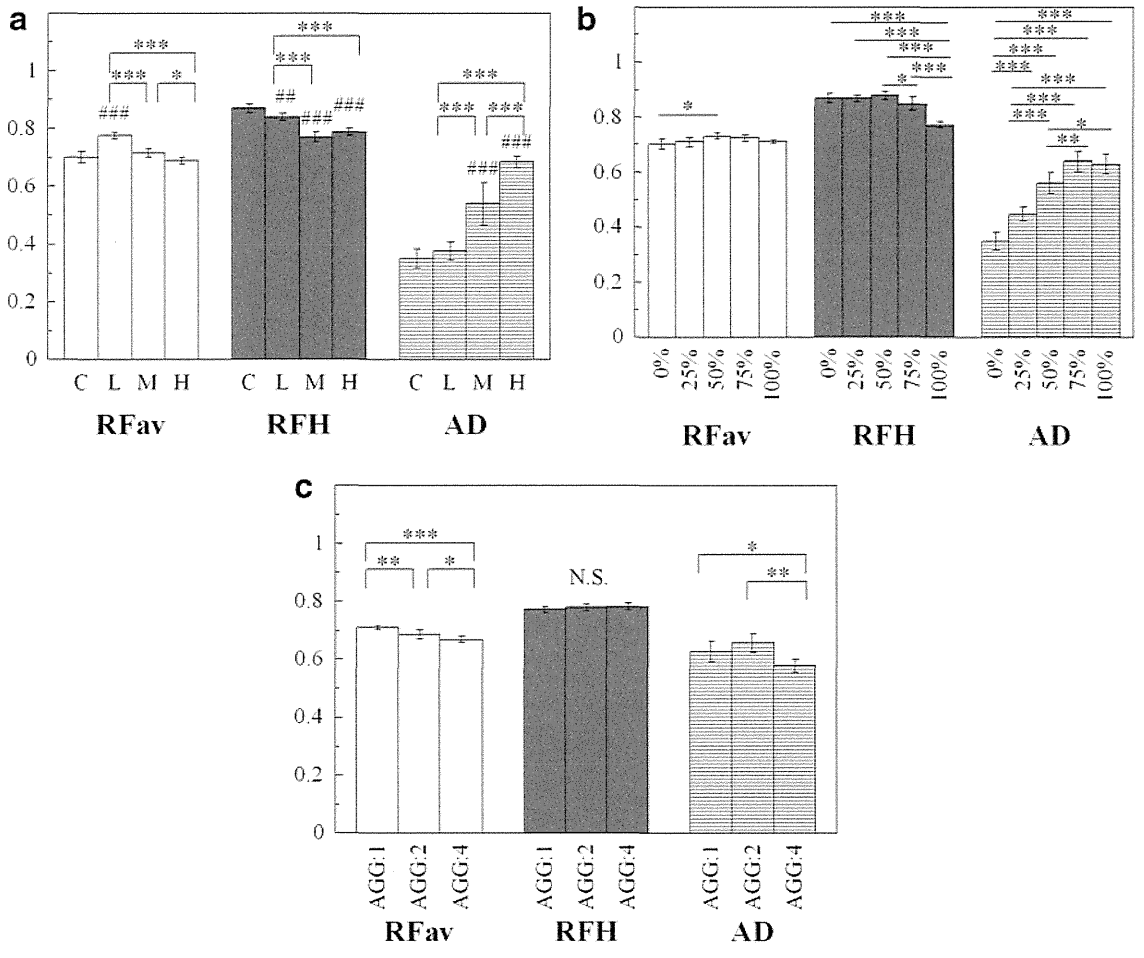

FIG. 4. Derived round factor average (RFav), roundness factor homogeneity (RFH), and area disorder (AD) from model type A [**(a)** differ in cell density], model type B [**(b)** differ in aggregate participation], and model type C [**(c)** differ in aggregate size]. In **(a)**, $^{*,\#}p < 0.05$, $^{\#\#}p < 0.01$, $^{***,\#\#\#}p < 0.001$; by Tukey–Kramer test. *Indicates significance between model groups, and #indicates significance between model groups and control groups. In **(b)** and **(c)**, $^{*}p < 0.05$, $^{**}p < 0.01$, $^{***}p < 0.001$; by Tukey–Kramer test. Error bars indicate square distributions; $n = 6$.

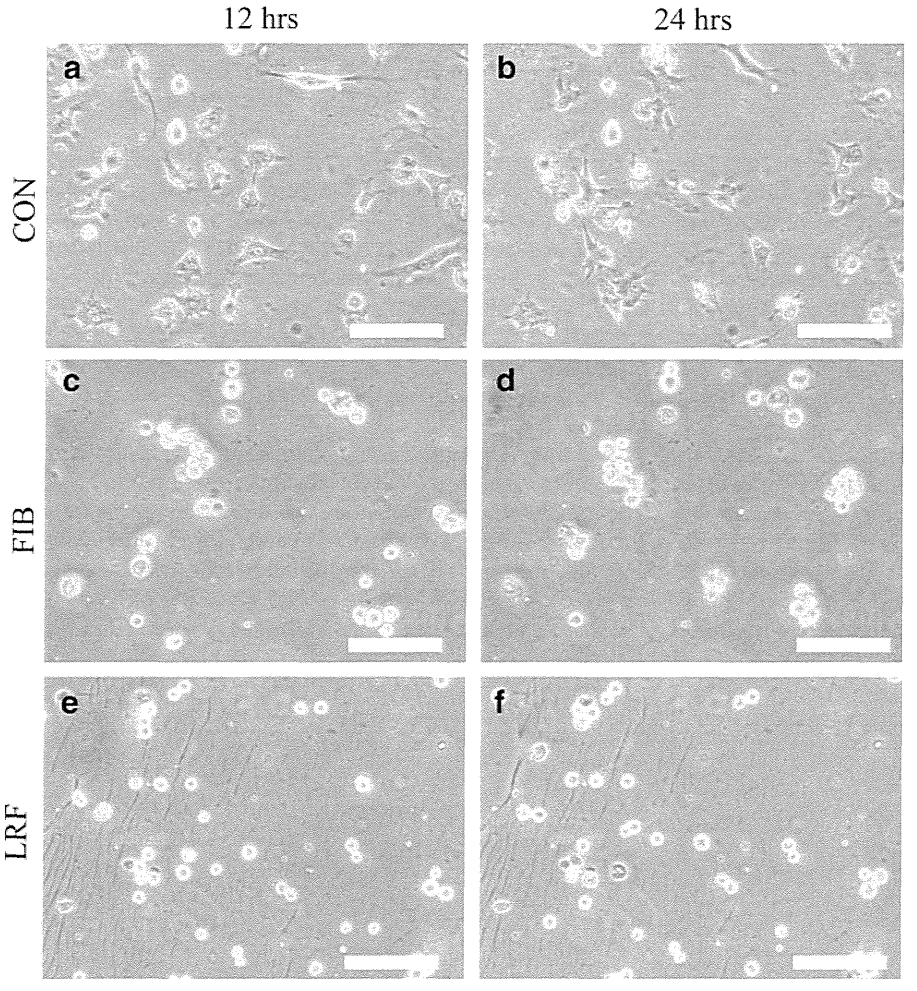

FIG. 5. Phase-contrast images of chondrocytes cultured on collagen **(a, b)**, on wild-type fibroin **(c, d)**, and on RGD fibroin surfaces **(c, f)**, which were taken 12 h **(a, c, e)** and 24 h **(b, d, f)** after seeding. Scale bar = 20 μm.

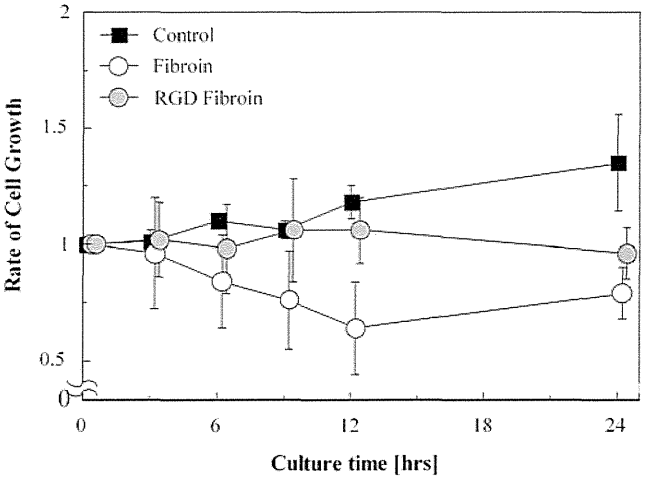

FIG. 6. Temporal changes in chondrocyte growth rate on each substrate. The significant change in the number of observed chondrocytes was seen only on the collagen surface by one-way analysis of variance. Error bars indicate square distributions; $n = 3$.

CON substrates was probably caused by the cells lack of aggregation. Asymptotic exponential curves were fitted to the mean values of the AD index in a time-dependent manner for every substrate (Fig. 8) The relaxation time was 1.56 for the FIB substrate and 4.39 for the LRF substrate, and the AD values for the FIB and LRF substrates were fixed at 0.54 and 0.49, respectively, during the 24-h culture period.

Discussion

The purpose of this study was to investigate how best to quantitatively characterize cell populations in various culture conditions. The results of simulation testing showed that RFav and RFH were insensitive to the rate at which cells participated in aggregation and the number of cells involved in aggregation, respectively. However, there appeared to be a direct relationship between AD and the degree of aggregation, with increasing AD values observed for increasing cell aggregation. The significance of this relationship was confirmed statistically (Tukey–Kramer test, $p < 0.05$). Using this information, the results of the *in vitro* experiments were analyzed and the cell aggregation behavior on the different substrates analyzed. According to the time-dependent changes in AD, the FIB surface seems to be quite different from the CON surface with respect to multicellular behavior.

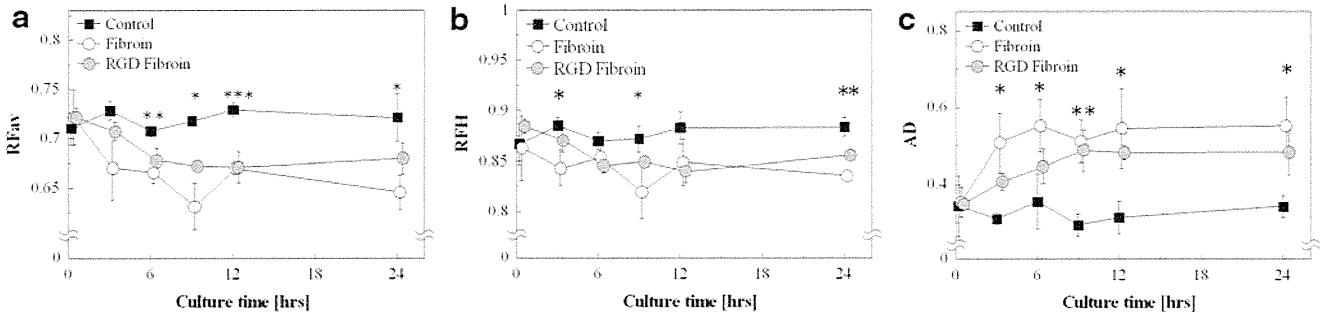

FIG. 7. Temporal changes in RFav **(a)**, RFH **(b)**, and AD **(c)** on each substrate. The significant changes were observed on wild-type fibroin for RFav ($p<0.01$) and AD ($p<0.01$) and on RGD fibroin for RFav ($p<0.001$), RFH ($p<0.001$), and AD (0.05). All three indexes exhibited no significant change on the collagen surface. *indicates significance between control and fibroin groups. *$p<0.05$, **$p<0.01$, ***$p<0.005$; by t-test. Error bars indicate square distributions; $n=3$.

Promotion of cell aggregation seems to be one of the characteristics of FIB substrates, and has been reported in other studies as well.[3,5] Using observational techniques, it is easy to qualitatively distinguish the differences between CON and FIB surfaces with respect to chondrocyte migration and population (Fig. 5a, b). However, it is quite difficult to determine whether wild-type FIB is different from RGD fibroin in terms of cell population, because this difference is too subtle to discern simply from observing photographic evidence (Fig. 5b, c). In that respect, the quantitative results of this study have demonstrated that multicellular behavior is affected by the coating substrate material, and have revealed different time-dependent processes.

There are few criteria for evaluating aggregated cell populations using a Voronoi diagram; so, three typical sets of cell population distribution were conducted in a simulation experiment. In the aggregation distribution model, all three indexes (AD, RFav, and RFH) changed according to the degree of cell density (type A), the degree of cell participation in aggregating (type B), and the number of cells in a single aggregate (type C). In types A and B, as the cells came closer to each other or as more cells became more aggregated, the cell density gap increased between crowded and barren areas, and subsequently led to an increase in AD and a decrease in RFH. Similarly, Marcelpoil and Usson suggested that an increase in AD signifies populations containing aggregates in particular locations, whereas a decrease in RFH signifies populations containing barren islets.[12] Moreover, Nawrocki Raby *et al.* defined the shift from initial distribution toward clustering as the increase of AD (from 0.33 to 0.57) in conjunction with the decrease of RFH (from 0.80 to 0.77).[9] In the *in vitro* experiments, AD, on average, increased significantly from 0.35 ± 0.04 to 0.55 ± 0.07 and from 0.35 ± 0.02 to 0.48 ± 0.06 for FIB and LRF substrates, respectively. On the other hand, RFH, on average, was decreased from 0.86 ± 0.032 to 0.84 ± 0.003 and from 0.88 ± 0.007 to 0.86 ± 0.002 for FIB and LRF substrates, respectively. Even though, RFH decreased for both FIB and LRF substrates, statistical significances were detected only for LRF.

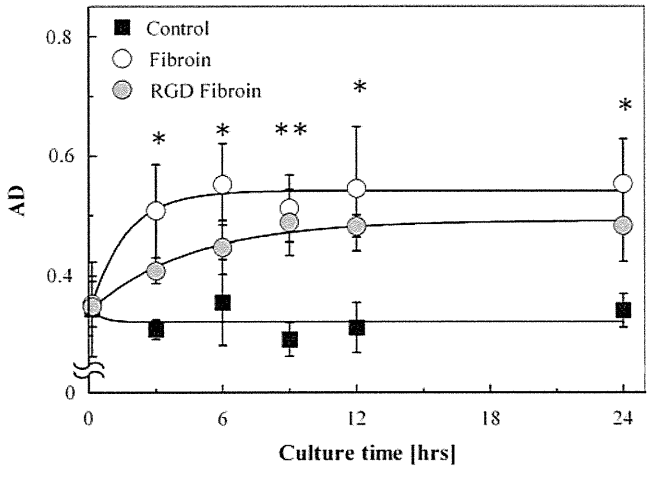

FIG. 8. Regression analysis of temporal AD changes for each substrate, resulting in a fit with R^2 of 0.13 (collagen), 0.96 (wild-type fibroin), and 0.99 (RGD fibroin). Each AD value converged to 0.32, 0.54, and 0.49, with a relaxation time of 0.44, 1.56, and 4.39 h, on collagen, wild-type fibroin, and RGD fibroin, respectively. *indicates significance between control and fibroin groups. *$p<0.05$, **$p<0.01$; by t-test.

There is one considerable reason why RFH did not change significantly. When less than half of the cells are in aggregation in simulation model type B, RFH values remain around 0.76, whereas RFH sensitively decreases when more than half of the cells are aggregated. In addition, it seems that cell density in a cluster can also affect RFH values. Based on the results above, the RFH index varies only in the latest phase of aggregation process when a majority of cells come close to each other. On the other hand, the AD index increases gradually with cell aggregation in model types A and B. So, as far as evaluating chondrocyte aggregation on FIB surfaces (like in Fig. 5), AD is more appropriate than RFH. In fact, temporal changes in AD matched well with the qualitative impressions observed experimentally.

The degree of aggregate formation has been expressed subjectively in the histomorphology field. The AD index seems to best characterize cell-aggregate populations among the three indexes of the Voronoi Diagram under the hypotheses that positive correlation with models A (H, M, and L) and B (0%, 25%, 50%, 75%, and 100%) together with no correlation with model C (AGG1, AGG2, and AGG3) agrees with the subjective criteria for aggregation. From time-lapse microscopy, most events in cell aggregation were observed during the first 12 h after seeding, with cell migration subsequently normalizing, followed by cell–cell adhesion. From this analysis, chondrocyte aggregation was supposed to be a relaxation process; hence, regression analysis was performed

to fit the temporal AD changes recorded for each substrate into an asymptotic exponential model. As a result, the decrease in relaxation time between FIB and LRF suggests that regression analysis of AD can be used to assess whether culture substrates can affect the cell aggregation process. Interestingly, the aggregation speed was delayed from 1.56 to 4.39 h on the RGDSx2 peptide interfused FIB substrate.

An RGD amino acid sequence is the minimum unit of a cell–substrate adhesive activity domain, which is a ligand of integrin.[15,16] Ryan *et al.* reported that decreasing substratum adhesiveness might lead to a slower rate of cell aggregation spreading over the substrate.[17] Moreover, Briggs *et al.* reported that the weakening of cell–substrate adhesion and the formation of cell aggregates were observed simultaneously and also accompanied the osteogenic differentiation of mesenchymal stem cells.[18] These results suggest that a balance between cell–cell and cell–substrate adhesion is one of the important factors in predicting cell aggregate formation/deformation. On the other hand, Kambe *et al.* reported that RGDSx2 peptide interfused into silk FIB significantly increased the cell adhesive force until 12 h after seeding.[19] Taking the above into consideration, it may be possible that cell–substrate adhesiveness decreases the tendency and speed of chondrocyte aggregate formation as the adhesive force of FIB increases.

AD analysis may be able to evaluate the motility of cellular aggregates, especially with respect to speed, which is not measured in qualitative observation. However, there are many hurdles that still remain to be cleared before this method is ready for use in tissue engineering. One of the most important problems that need to be addressed is how to translate multicellular behavior indices into design criteria for biological tissue growth. Certainly, the mechanisms underlying regeneration processes are regulated by not only by cytoskeletal-mediated force transmission factors, such as integrin and cadherin, but also by a network of genetic or biochemical signaling pathways. For the FIB scaffold design, it is still unclear how the chondrocyte aggregation process affects the maintenance of the cartilaginous phenotype during tissue regeneration; hence, genetical or histological surveys are needed in future studies. Moreover, cell aggregation must be assessed carefully, because cell motility and cohesion are phenomena that are central to cell organization within tissue scaffolds. Lauffenburger *et al.* stated that maximally useful engineering design principles for cell organization within tissue structures will require the most comprehensive models for cell motility behavior to be able to predict multicellular organization from quantifiable characteristics of cell–matrix and cell–cell interactions.[20] In this respect, AD is an unrefined, but easy-to-use tool for characterizing cell aggregation, and can be one of the approaches used to investigate spatiotemporal characteristics of cell–matrix and cell–cell interactions.

Conclusions

The findings obtained from this study are the following: (1) Three indexes (RFav, RFH, and AD) of the Voronoi diagram identified the differences in spatiotemporal changes between chondrocytes grown on FIB and CON surfaces; (2) The regression analysis of the AD index revealed the speed of cells during aggregation; and (3) Transgenic RGDS sequences reduced the aggregate formation of chondrocytes cultured on FIB.

Acknowledgments

We would like to thank Alex Turner for helping to improve the manuscript; the Kyoto University Venture Business Laboratory and the Institute for Frontier Medical Sciences of Kyoto University for use of their facilities. This work was supported by the Grant-in-Aid for the Creative Scientific Research from the Japan Science and Technology Agency; the Agri-Health Translational Project from the Ministry of Agriculture, Forestry and Fisheries, Japan; and the Student venture support system grant from the Advanced Scientific Technology and Management Research Institute of Kyoto.

Disclosure Statement

No competing financial interests exist.

References

1. Terryn, C., Bonnomet, A., Cutrona, J., Coraux, C., Tournier, J.-M., Nawrocki-Raby, B., *et al.* Video-microscopic imaging of cell spatio-temporal dispersion and migration. Crit Rev Oncol Hematol **69,** 144, 2009.
2. Liu, W.F., and Chen, C.S. Cellular and multicellular form and function. Adv Drug Deliv Rev **59,** 1319, 2007.
3. Kawakami, M., Tomita, N., Shimada, Y., Yamamoto, K., Tamada, Y., Kachi, N., *et al.* Chondrocyte distribution and cartilage regeneration in silk fibroin sponge. Biomed Mater Eng **21,** 53, 2011.
4. Kim, M.-H., Kino-oka, M., Morinaga, Y., Sawada, Y., Kawase, M., Yagi, K., *et al.* Morphological regulation and aggregate formation of rabbit chondrocytes on dendrimer-immobilized surfaces with D-glucose display. J Biosci Bioeng **107,** 196, 2009.
5. Kachi, N.D., Otaka, A., Sim, S., Kuwana, Y., Tamada, Y., Sunaga, J., *et al.* Observation of chondrocyte aggregate formation and internal structure on micropatterned fibroin-coated surface. Biomed Mater Eng **20,** 55, 2010.
6. Martinez Mozos, O., Bolea, J.A., Ferrandez, J.M., Ahnelt, P.K., and Fernandez, E. V-Proportion: a method based on the Voronoi diagram to study spatial relations in neuronal mosaics of the retina. Neurocomputing **74,** 418, 2010.
7. Minciacchi, D., Kassa, R.M., Del Tongo, C., Mariotti, R., and Bentivoglio, M. Voronoi-based spatial analysis reveals selective interneuron changes in the cortex of FALS mice. Exp Neurol **215,** 77, 2009.
8. Bigras, G., Marcelpoil, R., Brambilla, E., and Brugal, G. Cellular sociology applied to neuroendocrine tumors of the lung: quantitative model of neoplastic architecture. Cytometry **24,** 74, 1996.
9. Nawrocki Raby, B., Polette, M., Gilles, C., Clavel, C., Strumane, K., Matos, M., *et al.* Quantitative cell dispersion analysis: new test to measure tumor cell aggressiveness. Int J Cancer **93,** 644, 2001.
10. Zahm, J.M., Hazgui. S., Matos, M., Ben Seddik, A., Nawrocki Raby, B., Polette, M., *et al.* Quantitative videomicroscopic analysis of the sociologic behavior of non-invasive and invasive tumor cell lines. Cell Mol Biol **52,** 54, 2006.
11. Matos, M., Nawrocki Raby, B., Zahm, J.-M., Polette, M., Birembaut, P., and Bonnet, N. Cell migration and proliferation are not discriminatory factors in the *in vitro* sociologic

behavior of bronchial epithelial cell lines. Cell Motil Cytoskeleton **53,** 53, 2002.
12. Marcelpoil, R., and Usson, Y. Methods for the study of cellular sociology: Voronoi diagrams and parametrization of the spatial relationships. J Theor Biol **154,** 359, 1992.
13. Tamura, T., Thibert, C., Royer, C., Kanda, T., Abraham, E., Kamba, M., *et al.* Germline transformation of the silkworm *Bombyx mori* L. using a piggyBac transposon-derived vector. Nat Biotechnol **18,** 81, 2000.
14. Aoki, H., Tomita, N., Morita, Y., Hattori, K., Harada, Y., Sonobe, M., Wakitani, S., and Tamada, Y. Culture of chondrocytes in fibroin-hydrogel sponge. Biomed Mater Eng **13,** 309, 2003.
15. Ruoslahti, E., and Pierschbacher, M.D. Arg-Gly-Asp: a versatile cell recognition signal. Cell **44,** 517, 1986.
16. Ruoslahti, E., and Pierschbacher, M.D. New perspectives in cell adhesion: RGD and integrins. Science **238,** 491, 1987.
17. Ryan, P., Foty, R., Kohn, J., Steinberg, M.S.. Tissue spreading on implantable substrates is a competitive outcome of cell-cell vs. cell-substratum adhesivity. Proc Natl Acad Sci U S A **98,** 4323, 2001.
18. Briggs, T., Treiser, M.D., Holmes, P.F., Kohn, J., Moghe, P.V., and Arinzeh, T.L. Osteogenic differentiation of human mesenchymal stem cells on poly (ethylene glycol)-variant biomaterials. J Biomed Mater Res A **91,** 975, 2009.
19. Kambe, Y., Yamamoto, K., Kojima, K., Tamada, Y., and Tomita, N. Effects of RGDS sequence genetically interfused in the silk fibroin light chain protein on chondrocyte adhesion and cartilage synthesis. Biomaterials **31,** 7503, 2010.
20. Lauffenburger, D.A., and Griffith, L.G. Who's got pull around here? Cell organization in development and tissue engineering. Proc Natl Acad Sci U S A **98,** 4282, 2001.

Address correspondence to:
Naohide Tomita, MD, PhD
C3b s01 Graduate School of Engineering
Kyoto University
Kyoto daigaku-Katsura
Nishikyo-ku
Kyoto 615-8540
Japan

E-mail: tomita.naohide.5c@kyoto-u.ac.jp

Received: July 12, 2012
Accepted: October 16, 2012
Online Publication Date: January 31, 2013